Radical Scavenger Properties of Oxide Nanoparticles Stabilized with Biopolymer Matrix

CRISTINA ILEANA COVALIU[1], CRISTIAN MATEI[1], SIMONA LITESCU[2], SANDRA ANA-MARIA EREMIA[2], NICOLAE STANICĂ[3], LUCIAN DIAMANDESCU[4], ADELINA IANCULESCU[1], IOANA JITARU[1], DANIELA BERGER[1*]

[1] University "Politehnica" of Bucharest, Faculty of Applied Chemistry and Materials Science,1-7 Polizu street, Bucharest 1, 011061, Romania

[2]National Institute for Biological Sciences, Centre of Bioanalysis, Bucharest 060031, Romania

[3]Romanian Academy, I.G. Murgulescu, Institute of Physical Chemistry, 202, Splaiul Independentei, 060021, Bucharest, Romania

[4]National Institute Of Materials Physics, Atomistilor 105 Bis, Bucharest, Romania

Nanoxide based composites are suitable materials for advanced medical application. Fe_3O_4, $CoFe_2O_4$ and MnO_2 nanoparticles, synthesized by different soft chemistry routes (precipitation in the presence of soft template and solution combustion) were coated by a biocompatible polymer, sodium alginate. The oxides and corresponding composites were structural and morphological characterized. The saturation magnetization for Fe_3O_4-based composite is 10.1 emu·g^{-1}, resulting magnetic domains of 5.2 nm that suggests a superparamagnetic property. Radical scavenging capability of the composites was investigated by two different methods, Trolox Equivalent Antioxidant Capacity (TEAC) and peroxide-chronoamperometry.

Keywords: ferrites, MnO_2, oxide-based composites, biopolymer matrix, radical scavenger

Functionalized magnetic particles from nanometer to micrometer scale could be used as contrast agents in magnetic resonance imaging (MRI) [1-4], in tissue repairing [4], detoxification of biological fluids [6], hyperthermia [7], drug delivery [8,9], cell separation [9] etc. The important properties of magnetic particles for medical applications are nontoxicity, biocompatibility, injectability, and high-level accumulation in the target tissue. Magnetic nanoparticles can also be used for drug targeting and bioseparation including cells sorting. Three different types of stabilization of magnetic particles for medical uses can be applied [10]: (*i*) by coating the magnetic particles with suitable surfactant (dextran, PVA), (*ii*) by obtaining nanocomposites consisting in a magnetic core and a nonmagnetic coating based on polysaccharide-type polymer [4,8], [$SiO_{1.5\gamma}$-$(CH_2)_3(NH_2)$] coating layer [11] etc and (*iii*) the formation of liposome-like vesicles filled with magnetic particles [10]. Polymers suitable for the synthesis of magnetic particle-based nanocomposites are: poly(alkylcyanoacrylates), poly(methylidene malonate), poly(lactic acid), poly(glycolic acid), [10] poly(amide-hydroxyurethane) [12] etc.

A polysaccharide-type polymer used as biocompatible coating is sodium alginate (ANa) that is extracted from brown algae. It is a linear polymer composed of α-*L*-guluronate and β-*D*-mannuronate units in different proportion.

The paper deals with the synthesis and characterization of Fe_3O_4, $CoFe_2O_4$ and MnO_2 particles coated with a biocompatible polymer, sodium alginate. We have investigated the magnetic properties and radical scavenger capacity of prepared composites.

When addressed the 'antioxidant' definition usually refers to compounds able to delay or to end the reaction of a substrate with a reactive species of oxygen [13]. Evaluation of antioxidant efficiency against oxidative stress is a demanding task due to all parameters that should be considered when the assessment of the effect is performed, namely: various method are used and the obtained results are expressed via different values of efficiency, as Trolox (6-hydroxy-2,5,7,8-tetramethylchroman-2-carboxylic acid) equivalent antioxidant capacity, TEAC (micromolar) [14], IC50 [15], or as induced peroxidation lag-phase etc. We have evaluated the radical scavenger properties of the composites by TEAC and by a chronoamperometric method, against H_2O_2. From our best knowledge this method was applied for the first time, to H_2O_2 – nanocomposite systems.

Experimental part

The composites have been obtained by two steps procedure. Firstly, the oxide nanoparticles have been prepared and then they have been coated with sodium alginate polymer. All chemicals (of analytical grade) are supplied from Sigma Aldrich (or Scharlau) and are used as received.

Synthesis of Fe_3O_4, $CoFe_2O_4$ and MnO_2 nanoparticles

Fe_3O_4 nanoparticles were prepared by coprecipitating Fe^{2+} and Fe^{3+} ions from corresponding 0.5 M aqueous solution by adding 28% ammonia solution in the presence of polyethylene glycol 200 (PEG200) as soft template, at room temperature. The molar ratio, Fe^{2+}: Fe^{3+}: PEG unit was 1:2:15. The *p*H of reaction mixture was kept at 12. Fe_3O_4 nanoparticles were separated by centrifugation and washed with water and ethanol.

$CoFe_2O_4$ nanoparticles were obtained by combustion method using corresponding metallic nitrates and α-alanine in fuel rich conditions (20% excess of α-alanine). More details about the synthesis and cobalt ferrite structure evolution were presented elsewhere [16]. $CoFe_2O_4$ powder obtained at 400°C as single-phase compound with inverse spinel structure and cubic symmetry was used to prepare the composite.

MnO_2 nanoparticles were prepared in a two steps procedure. Pure crystalline Mn_3O_4 with hausmanit structure and tetragonal symmetry was obtained by direct precipitation of 0.2 M aqueous solution of manganese

* email: danaberger@yahoo.com, tel: 0214023986

nitrate with 0.5 M aqueous solution of sodium hydroxide in the presence of polyvinylpyrrolidone, PVP, (molar ratio, Mn^{2+}: PVP unit, 1:5) as soft template. The pH of reaction mixture was kept at 10. The precipitate was ageing at 75°C for 24 h under vigorous magnetic stirring. Mn_3O_4 powder was separated by centrifugation, washed several times with water and dried in air at 105 °C for 2 h. MnO_2 was obtained after a long treatment of Mn_3O_4 in 50% aqueous solution of H_2SO_4 at 80°C.

Synthesis of Fe_3O_4-ANa, $CoFe_2O_4$-ANa and MnO_2-ANa nanocomposites

All three composites were obtained using the same procedure presented elsewhere [16]. The oxide nanopowder (20% wt.) was added to 1% aqueous solution of sodium alginate polymer. The uncoated nanoparticles were separated by centrifugation.

The oxide nanopowders were characterized by X–ray diffraction (XRD), FTIR spectroscopy and scanning electron microscopy (SEM) and the nanocomposites were investigated by atomic absorption spectroscopy (AAS), XRD, FTIR, Mössbauer spectroscopy and SEM. XRD patterns were obtained on a RIGAKU Miniflex II diffractometer with CuKα radiation. FTIR spectra were performed on BRUKER Tensor 27 spectrometer and SEM images were acquired on a PHILIPS Quanta Inspect F with field emission gun or HITACHI S2600 scanning electron microscope. The Mössbauer spectra were recorded at room temperature in the standard transmission geometry, using a 25 mCi, ^{57}Co in rhodium matrix and a spectrometer in transmission geometry with a Wiesel data acquisition system. The velocity calibration was performed with a standard alpha iron foil. The computer fit was performed in the hypothesis of Lorentzian shape of the absorption lines. The oxide particles content in the composite was determined by using ANALYTIK JENA Atomic Absorption Spectrophotometer Contra AA7. The magnetic measurements were carried out on Faraday-type magnetometer.

Two different methods to evaluate the antioxidant capacity, more exact radical scavenging capacity, of composites were used. The first one was a classical method, based on Trolox Equivalent Antioxidant Capacity (TEAC) assay, which consists in determination of the radical scavenging properties of composite against ABTS (2,2'-azino-bis(3-ethylbezthiazoline-6-sulphonic acid) cation radical. The method is spectrometric (UV-Vis spectrometer ABLE JASCO 550), based on the decay of 734 nm maximum absorbance of ABTS cation radical ($ABTS^{+\cdot}$) measured in the presence of presumed antioxidant composite. The cation radical $ABTS^{+\cdot}$ was generated as follows: 7 mM solution ABTS is prepared in 2.5 mM $K_2S_2O_8$ solution and allowed to interact at least 4-6 h, in dark, in order to stabilize the cation radical $ABTS^{+\cdot}$ formation. The results were addressed as Trolox equivalent, using the formula given in equation (2). Trolox (6-hydroxy-2,5,7,8-tetramethylchroman-2-carboxylic acid) was chosen due to the fact that is the general accepted reference antioxidant compound when determinations are performed in water based systems, being highly stable with respect to other known antioxidants (like ascorbic acid).

$$TEAC_{sample} = C_{Trolox} \cdot f \cdot \frac{A_{sample} - A_{blank}}{A_{Trolox} - A_{blank}} \qquad (1)$$

where:

A_{blank} represents the absorbance, measured at 20 min after addition of 2500 µL of 0.0175 mM $ABTS^{+\cdot}$ solution, in a UV-Vis cuvette containing 500 mL ultrapure water. A_{Trolox} represents the absorbance measured at 20 min after addition of 100 µL Trolox 0.01 mM solution and 400 µL ultrapure water to a 2500 µL $ABTS^{+\cdot}$ 2.5 mM. A_{sample} represents the absorbance, measured at 20 min after addition of 100 µL of sample suspension (33.33 $mg \cdot L^{-1}$) to 2500 µL of $ABTS^{+\cdot}$ 2.5 µM solution and 400 µL ultrapure water. C_{Trolox} is the effective concentration of Trolox ($\mu mol \cdot L^{-1}$) and f is the dilution factor of the sample. The reaction time was established to 20 min considering the stability of $ABTS^{+\cdot}$ maximum absorbance and the sample (nanocomposite) specificity.

The second method to evaluate the antioxidant capacity of the composites was a chronoamperometric method (UNISCAN PG580 potentiostat), consisting in measuring the amount of hydrogen peroxide scavenged by the tested composite samples. The measurements were performed at +650 mV vs Ag/AgCl reference electrode, in a three electrodes electrochemical cell, using a Pt (d=1 mm) working electrode and a Pt wire counter electrode. The difference between the current intensity obtained for a certain concentration of hydrogen peroxide (in our experiments a concentration of 100 $\mu mol \cdot L^{-1}$ was used, the concentration being established after the calibration of the electrode response against H_2O_2) in the absence of presumed antioxidants and the current intensity obtained for the same concentration of hydrogen peroxide in the presence of composite is proportionally correlated with the amount of scavenged H_2O_2 by the tested sample.

Results and discussions

The interactions between oxide particles and sodium alginate polymer were studied by FTIR spectroscopy (fig. 1). The broad band of 3100-3524 cm^{-1} is assigned to the symmetric and asymmetric stretching vibrations of OH groups [17].

The presence of this band in all the spectra of pristine oxide nanoparticles suggests the presence of superficial OH groups. The bands of 1014 cm^{-1} (fig. 1a), 1039 cm^{-1} (fig. 1b) and 1031 cm^{-1} (fig. 1c), respectively were assigned to the stretching modes of C-OH bonds, whereas the band from 1404 cm^{-1} (fig. 1a), 1415 cm^{-1} (fig. 1b) and 1408 cm^{-1} (fig. 1c), respectively correspond to $\nu_s(COO^-)$. It could be noticed that the band at 1590 cm^{-1} assigned to $\nu_{as}(COO)$ in sodium alginate spectrum (fig. 1d) is shifted to lower values, 1587 cm^{-1}, in the spectrum of MnO_2-ANa composite (fig. 1c) and to higher values 1608 cm^{-1} and 1609 cm^{-1} in the case of Fe_3O_4-ANa (fig. 1a) and $CoFe_2O_4$-ANa (fig. 1b), respectively, which suggests that sodium alginate carboxylate groups have reacted with superficial hydroxyl groups of oxide nanoparticles. The characteristic vibration bands corresponding to metal-oxygen bonds are in the range of 400-800 cm^{-1} in the FTIR spectra of oxide powders, as well as for the composites [17].

The nanopowders and the corresponding nano-composites were structurally analyzed by XRD (fig. 2) and Mössbauer spectroscopy (fig. 3). XRD data of Fe_3O_4 synthesized by precipitation method show the formation of Fe_3O_4 single-phase compound (fig. 2a) with inverse spinel structure (ICDD 82-1533) and 8 nm the average crystallite size, calculated by Rigaku PDXL software. The XRD pattern of as-prepared $CoFe_2O_4$ annealed at 400 °C, 3h have proved the formation of $CoFe_2O_4$ single-phase compound with inverse spinel structure and cubic symmetry (ICDD 22-1086). The average crystallite size calculated for cobalt ferrite sample was 21 nm. In the case of manganese oxide nanoparticles, the XRD data have proved the formation directly in the precipitation step, crystalline Mn_3O_4, with hausmamite structure (ICDD 80-0382) and tetragonal symmetry (fig. 2c). MnO_2 as mixture of γ and ε phases

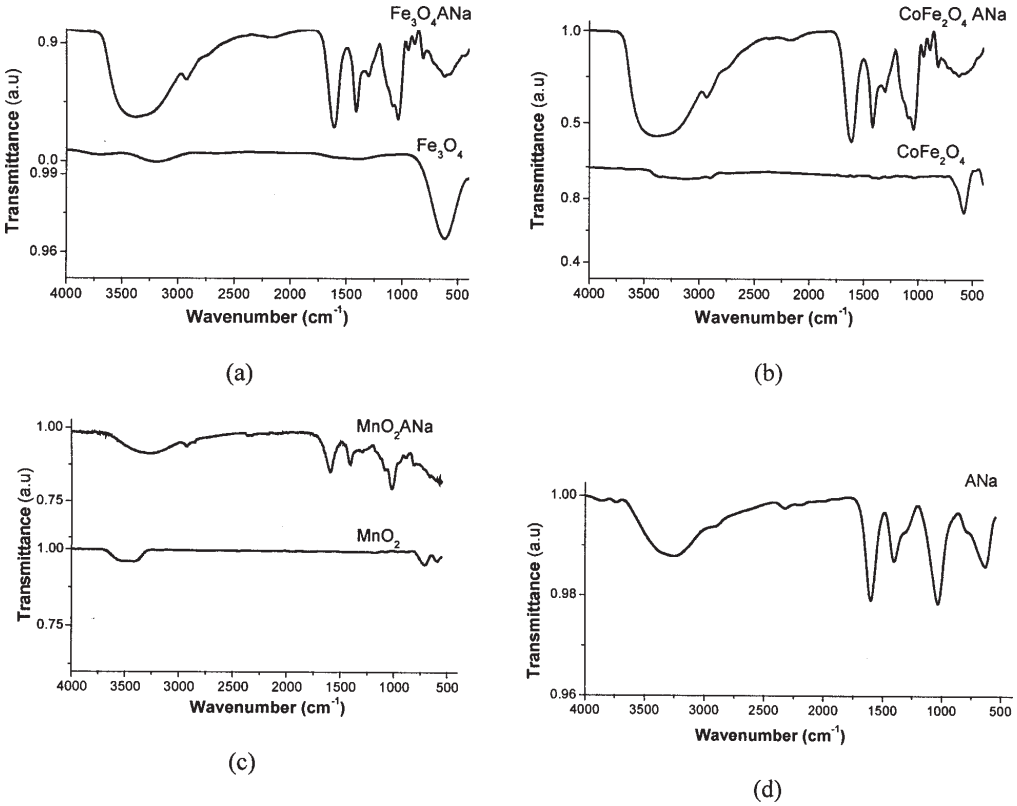

Fig. 1. FTIR spectra of the samples: Fe_3O_4 and Fe_3O_4ANa (a); $CoFe_2O_4$ and $CoFe_2O_4$ANa (b); MnO_2 and MnO_2ANa(c); ANa (d)

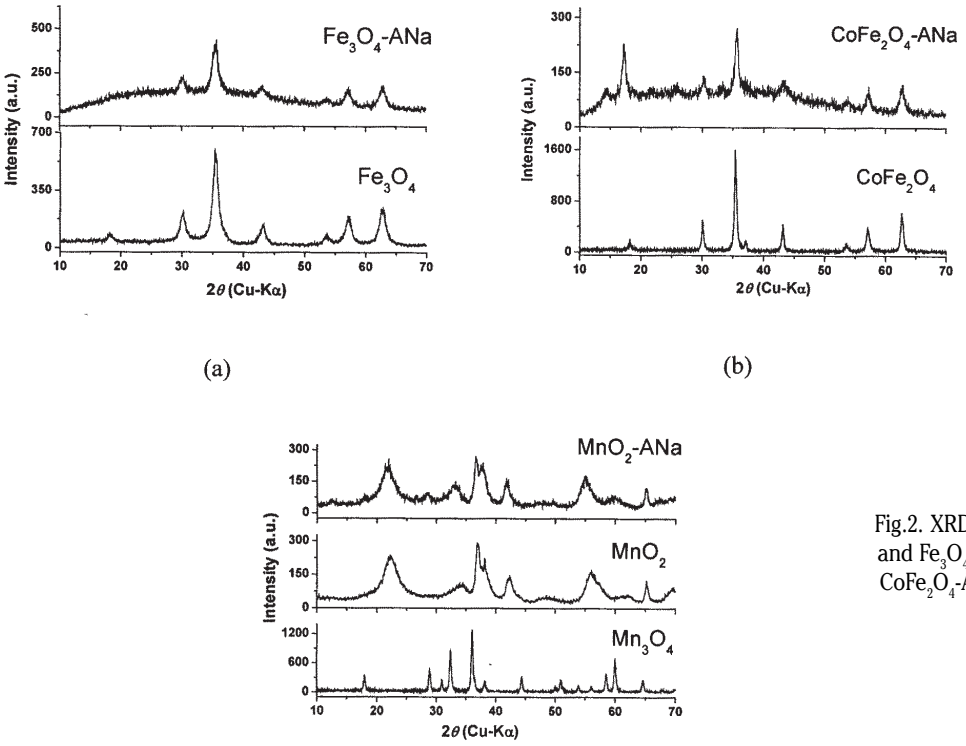

Fig.2. XRD patterns of: (a) Fe_3O_4 powder and Fe_3O_4-ANa; (b) $CoFe_2O_4$ powder and $CoFe_2O_4$-ANa; (c) synthesized MnO_2 and MnO_2Ana

was obtained subsequently to a long treatment of Mn_3O_4 powder in 50% H_2SO_4 solution. The average crystallite size calculated for hausmanite phase was 28.6 nm and 7 nm for MnO_2, respectively. This difference indicates that the oxidation of Mn_3O_4 by H_2SO_4 treatment is a complex process. The XRD patterns of all the composites indicate that the crystalline structure of the oxides nanoparticles is preserved after the coating procedure (fig. 2).

The Mössbauer spectrum of Fe_3O_4-ANa composite (fig. 3a) exhibit the characteristic [18] two magnetic patterns of Fe_3O_4 with hyperfine magnetic field of 49.3 T for the tetrahedral positions of iron ((1) in fig. 3a) and 45.7 T for the octahedral ones ((2) in fig. 3a). The relative area of these two magnetic sublattices is close to 2/3 which is the typical value for the stoichiometric magnetite. A small doublet is present in the central part of the spectrum. The relative abundance is less than 4 %, but the origin of this doublet remains unknown.

The Mössbauer spectrum of $CoFe_2O_4$-ANa composite displays a magnetic hyperfine pattern. The cobalt ferrite is basically an inverse Fe^{3+} spinel, although the room temperature magnetic spectrum does not resolve tetrahedral and octahedral site hyperfine fields. The computer fit (continuous line in fig. 3b) gives a hyperfine

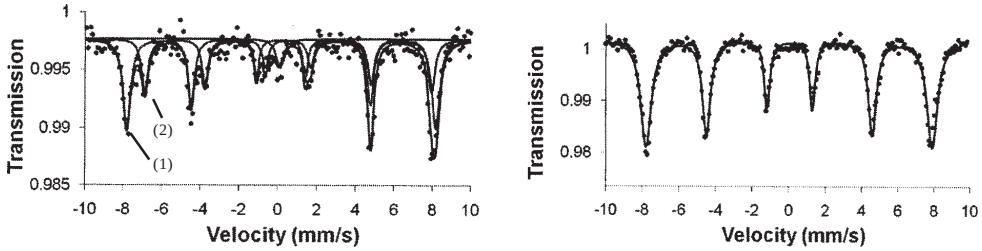

a) b)

Fig. 3 Mössbauer spectra of (a) Fe_3O_4 -ANa composite synthesized by forced hydrolysis and (b) $CoFe_2O_4$-ANa composite

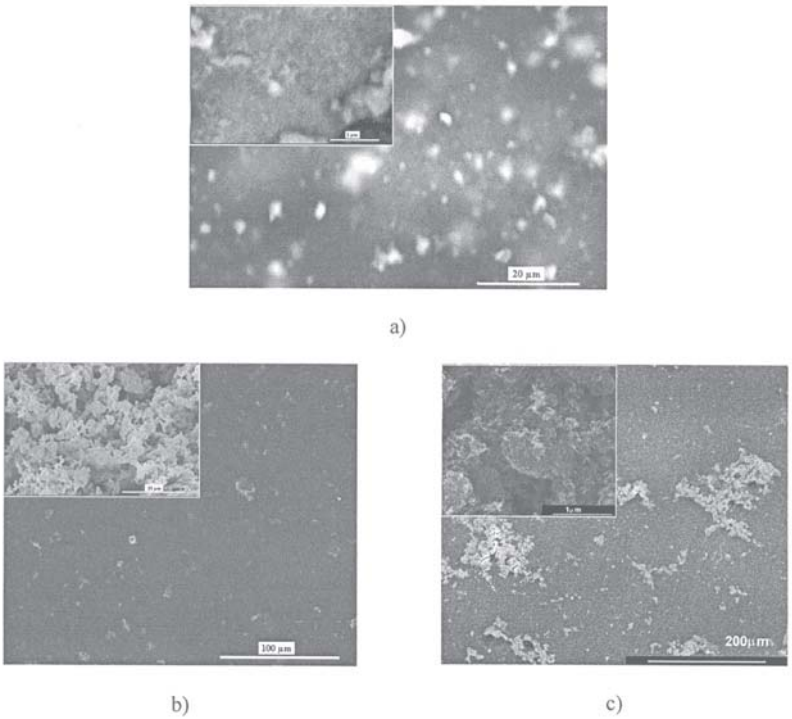

a) b) c)

Fig. 4. SEM micrographs of (a) Fe_3O_4-ANa; inset Fe_3O_4 powder; (b) $CoFe_2O_4$-ANa composite; inset $CoFe_2O_4$ powder; (c) MnO_2-ANa composite; inset MnO_2 powder

magnetic field of 491 HOe which is smaller than the bulk value of 516 [18] probably due to smaller particle size in the system.

The morphology of the composite samples has been investigated by SEM. Fe_3O_4 and $CoFe_2O_4$ powders with particles of spherical shape that form spongy and compact, respectively agglomerates are randomly distributed in the composite film (fig. 4a and 4b). The particles of MnO_2 with acicular shape and 80 nm average length form agglomerates with irregular shapes that are coated by sodium alginate (fig. 4c). The average sizes of the oxide particles and the agglomerates in the composites are presented in table 1.

The nanoparticles content of the composites was calculated from AAS analyses and the results are presented in table 1. It could be noticed that the content of the nanoparticles in the composites is directly related to the particles size, but unexpected, independent from the agglomerates size.

The magnetization data obtained for Fe_3O_4-ANa composite are well described by the Langevin function, and the saturation magnetization for this sample was found 10.1 emu·g^{-1} that correspond to 72 emu·g^{-1} for the Fe_3O_4 oxide particles. The value is smaller than 96 emu·g^{-1}, the saturation magnetization for "bulk" Fe_3O_4 and suggests the presence of very small magnetic domains. Assuming a spherical geometry for the particles, it was found an average size of 5.2 nm calculated from magnetic measurements, smaller than 8 nm, the crystallite size obtained from XRD. The small magnetic domains induce the superparamagnetic properties for the composite. This property, in conjunction with large agglomerates in

Compound	Oxide nanoparticles content (%)	Particle /agglomerate average size (nm) / (μm)	Crystallite average size (nm)
Fe_3O_4-ANa	14.1	300 / 3	8
$CoFe_2O_4$-ANa	9.9	150 / 10	21
MnO_2-ANa	9.1	80 / 150	7

Table 1
OXIDE NANOPARTICLES CONTENT, CRYSTALLITE, PARTICLE AND AGGLOMERATE SIZES IN THE COMPOSITE SAMPLES

Table 2
CHRONOAMPEROMETRIC DATA AND RADICAL SCAVENGER PROPERTIES OF THE SAMPLES VERSUS H_2O_2

No. crt.	Tested material	Δi (nA) ; (n=6)*	H_2O_2 scavenged ($\mu mol \cdot L^{-1}$)
1.	MnO_2	125.67	1.96
2.	MnO_2-ANa	35.01	1.31
3.	$CoFe_2O_4$	51.99	1.43
4.	$CoFe_2O_4$-ANa	104.33	1.81
5.	Fe_3O_4	49.96	1.42
6.	Fe_3O_4-ANa	107.00	1.83

*n- number of measurements

Δi- mean value of difference of registered current intensity

composites could be very important in MRI applications requiring a long retention contrast agent. The saturation magnetization obtained for $CoFe_2O_4$-ANa composite was found 6.83 $emu \cdot g^{-1}$ (69 $emu \cdot g^{-1}$ after the weight correction). This high value for saturation magnetization could be explained by the existence of large pure magnetic domains (larger than 10 nm) and it is in agreement with the crystallite size calculated from XRD and literature data [19].

If $CoFe_2O_4$ itself has no radical scavenging effect, the biocompatibilized $CoFe_2O_4$-ANa proved a TEAC value of 8.31 $\mu mol \cdot L^{-1}$, the observed effect being clearly associated to the alginate used to obtain the biocompatible composite. The same effect was noticed even for Fe_3O_4 that as nanoparticle has no radical scavenging effect against ABTS cation radical, while when biocompatibilized with alginate, shown a TEAC value of 77.89 $\mu mol \cdot L^{-1}$. When manganese nanoparticles were tested, for MnO_2 it was noticed that a TEAC value of 10.26 $\mu mol \cdot L^{-1}$ was obtained, a higher value being observed for the composite, namely 109.64 $\mu mol \cdot L^{-1}$. It could be clearly concluded that by biocompatibilization, the radical scavenging capacity against $ABTS^+$ of nanoparticles either is increased or starts to appear. It should be emphasized that nanoparticles covering with alginate generates a synergetic effect on revealed nanoparticles radical scavenging effect. Arguments sustaining this assertion are the values of TEAC obtained for composites that are higher than that obtained for alginate 5.41 ± 0.6 $\mu mol \cdot L^{-1}$ (n=5) itself or nanoparticles themselves, when determinations were performed on the concentration levels compatible to those used in composites synthesis.

When scavenged H_2O_2 was determined, the following equation of calibration for H_2O_2 response was used: Δi (nA) = 138.9xC ($\mu mol \cdot L^{-1}$) – 147.33 (R^2 = 0.9988). For tested samples the obtained results are given in the table 2, the measuring time was 10 min at room temperature.

As could be noticed, with the exception of MnO_2-ANa, all tested composites are more efficient radical scavengers for H_2O_2 than the pristine oxides. The differences of results obtained for TEAC and H_2O_2 assays in the case of MnO_2 and its composite should not be considered as artifacts, due to the fact that, as mentioned in the introduction part, there are not universal antioxidants, and consequently, some antioxidants are more efficient against some certain free radicals and less efficient against other free radicals, the efficiency that is related to structural features and to the measuring conditions.

Conclusions

Fe_3O_4, $CoFe_2O_4$ and MnO_2 – sodium alginate nanocomposites were exhaustively structurally and morphologically characterized. Fe_3O_4–ANa and $CoFe_2O_4$–ANa have exhibited enhanced antioxidant properties versus pristine oxides or sodium alginate polymer, proved by two different methods. The magnetic properties of Fe_3O_4-ANa and $CoFe_2O_4$-ANa recommend these materials for special MRI applications. By correlating the magnetic properties with the antioxidant properties, one can suggest the use of these composites as magnetic-vectored detoxification of the internal organs. Particularly, MnO_2-ANa composite has selective antioxidant capacity to different free radical generators and could be use in specific medical treatments.

Acknowledgment
This work was partially supported by the Romanian grant PNCDI II no. 62-053/2008 and CNCSIS grant TD 244/2007.

References

1.COROT, C., ROBERT, P., IDÉE, J.M., PORT, M., Recent advances in iron oxide nanocrystal technology for medical imaging, Advanced drug delivery reviews, **58**, 2006, p. 1471.
2.ZHAO, D.L., ZENG, X.W., XIA, Q.S., TANG, J.T., Preparation and coercivity and saturation magnetization dependence of inductive heating property of Fe_3O_4 nanoparticles in an alternating current magnetic field for localized hyperthermia, J. Alloy Comp., **469**, 2009, p. 215
3.LU, J., MA, S., SUN, J., XIA, C., LIU, C., WANG, Z., ZHAO, X., GAO, F., GONG, Q., SHUAI, X., AI, H., GU, Z., Manganese ferrite nanoparticle micellar nanocomposites as MRI contrast agent for liver imaging, Biomaterials, **30**, 2009, p.2919.
4.BAHADUR, D., GIRI, J., Ca alginate as scaffold for iron oxide nanoparticles synthesis, Biomaterials and Magnetism, **28**, 2003, p.639.
5.ALEXIOU, C., ARNOLD, W., KLEIN, R.J., PARAK, F.G., HULIN, P., BERGEMANN, C., ERHARDT, W., WAGENPFEIL, S., LUBBE, A.S., Locoregional Cancer Treatment with Magnetic Drug Targeting, Cancer Res., 60, 2000, p. 6641

6.GUPTA, A.K., GUPTA, M., Synthesis and surface engineering of iron oxide nanoparticles for biomedical applications, Biomaterials, 26, 2005, p. 3995
7.KIM, D.H., NIKLES, D.E., JOHNSON, D.T., BRAZEL, C.S., Heat generation of aqueously dispersed $CoFe_2O_4$ nanoparticles as heating agents for magnetically activated drug delivery and hyperthermia, J. Magn. Magn. Mater., **320**, 2008, p. 2390
8.WANG, Y.X., HUSSAIN, S.M., KRESTIN, G.P, Preparation and inductive heating property of Fe_3O_4–chitosan composite nanoparticles in an AC magnetic field for localized hyperthermia, Eur. Radiol. **11**, 2001, p. 2319
9.CHENG, F.Y., SU, C.H., YANG, Y. S., YEH, C.S., TSAIB, C.Y., WU, C.L., WU, M.T., SHIE, D.B., Characterization of aqueous dispersions of Fe_3O_4 nanoparticles and their biomedical applications, Biomaterials, **26**, 2005, p. 729
10.ITO, A., SHINKAI, M., HONDA, H., KOBAYASHI, T., Medical application of functionalized magnetic nanoparticles, J. Biosci. & Bioeng., **100**, 2005, p.1
11.OBREJA, L., DOROHOI, D.O., MELNIG, V., FOCA, N., NASTUTA, A., Mat. Plast., **45**, 2008, p.261
12.IORDACHE, P.Z., SOMOGHI, V., SAVU, I., PETREA, N., MITRU, G., PETRE, R., DIONEZIE, B., ORDEANU, V., HOTARANU, A., MUTIHAC, L, Mat. Plast., **46**, 2009, p.162
13.HALLIWELL, B., GUTTERIDGE, J.M.C., Antioxidant defenses: endogenous and diet derived in Free Radicals in Biology and Medicine. 4th Ed., Oxford University Press: Clarendon, 2007
14.RE, R., PELLEGRINI, N., PROTEGGENTE, A., PANNALA, A., YANG, M., RICE-EVANS, C., Antioxidant activity applying an improved ABTS radical cation decolorization assay, Free Rad. Biol. Med., **26**, 1999, p. 1231
15.FOTI, M.C., DAQUINO, C., GERACI, C., Free-radical-scavenging effect of carbazole derivatives on DPPH and ABTS radicals, J. Org. Chem., 69, 2004,p. 2309
16.COVALIU, C.I., MATEI, C., IANCULESCU, A., JITARU, I., BERGER, D., Fe_3O_4 and $CoFe_2O_4$ stabilized in sodium alginate polymer, U.P.B. Sci. Bull., Series B, **71**, 2009 (in press)
17.NAKAMOTO, K., Infrared and Raman Spectra of Inorganic and Coordination Compounds. Part B. John Wiley and Sons, New York, 1997
18.GREENWOOD, N.N., GIBB, T.C., Mössbauer Spectroscopy, Champman and Hall Ltd. London 1971
19.HAN, M.H., Development of Synthesis Method for Spinel Ferrite Magnetic Nanoparticle and its Superparamagnetic Properties, PhD thesis, Georgia Institute of Technology, 2008

Manuscript received. 2.11.2009